WPPFC-PR(18) 20290

C Li et al.

An in situ Diagnostic Method for Monitoring of Fuel Retention on the First Wall under Long-Pulse Operation of Experimental Advanced Superconducting Tokamak

Preprint of Paper to be submitted for publication in
Review of Scientific Instruments

An *in situ* Diagnostic Method for Monitoring of Fuel Retention on the First Wall under Long-Pulse Operation of Experimental Advanced Superconducting Tokamak

Cong Li[1,3], Dongye Zhao[1], Zhenhua Hu[2], Liying Sun[1], Niels Gierse[3], Dirk Nicolai[3], Ding Wu[1], Ping Liu[1], Ran Hai[1], Chunlei Feng[1], Fang Ding[2], Xi Jiang[3], Guang-nan Luo[2], Sebastijan Brezinsek[3], Christian Linsmeier[3], Yunfeng Liang[3], and Hongbin Ding[1,a)]

[1] *Key Laboratory of Materials Modification by Laser, Ion and Electron Beams, Chinese Ministry of Education, School of Physics, Dalian University of Technology, 116024 Dalian, P.R. China*

[2] *Institute of Plasma Physics, Chinese Academy of Sciences, P.O. Box 1126, 230031 Hefei, P.R. China*

[3] *Forschungszentrum Jülich GmbH, Institut für Energie- und Klimaforschung - Plasmaphysik, Partner of the Trilateral Euregio Cluster (TEC), 52425 Jülich, Germany*

a)Author to whom correspondence should be addressed. E-mail: hding@dlut.edu.cn

ABSTRACT

Plasma-wall interaction (PWI) research is an active field of study in long-pulse operation in current magnetic confinement fusion devices, such as the Experimental Advanced Superconducting Tokamak (EAST). It is an urgent requirement to be able to investigate several key PWI issues, such as fuel retention and material deposition, by *in situ* diagnostic methods. In this work, an *in situ* laser-induced breakdown spectroscopy (LIBS) system combined with an optical emission spectroscopy (OES) system and a flexible timing system is developed. The system is applied to study PWI during long-pulse plasma operation conditions in EAST. The timing system, as a core part of the diagnostic system, can control not only laser-related parameters like external triggers of laser flash lamp and Q-switch but also detection systems like spectrometer and camera sequence as well as time delay. This allows the system to monitor the edge plasma condition by OES as well as the first wall composition by LIBS in the long-pulse plasma operation in EAST, and then compare and combine the respective results. The results show that the spectral emission intensities of deuterium (D) and lithium (Li) from the edge plasma in the H-mode discharge are much stronger than in the ohmic discharge. Moreover, the emission intensity of the Dα signal is successfully measured and the signal is used to investigate the local particle flux and fluence. The preliminary results of fuel retention show that the amount of D retention on the first wall increases as the local edge D particle fluence increases. Particularly, the D retention is dominated and influenced by the local edge D particle fluence in long-pulse plasma discharges. Based upon the observation of Li emission in the LIBS in conjunction with D emission, Li-D codeposition could be the main source of fuel retention in EAST. Additionally, the design of an upgraded *in situ* LIBS endoscopic system is proposed which will enable monitoring of the upper divertor area and the strike zone in upcoming campaigns of EAST.

Keywords: plasma-wall interaction, fuel retention, tokamak, laser-induced breakdown spectroscopy

I. INTRODUCTION

Plasma-wall interaction (PWI) processes are important in long-pulse plasma operation fusion devices, such as the International Thermonuclear Experimental Reactor[1] (ITER), due to the main issues of increased fuel retention, material erosion and redeposition which are induced by a large increase in particle fluence to the wall compared to present experiments. In ITER, the in-vessel tritium inventory must be minimized and is limited to < 700 g due to the safety requirement.[2,3] Additionally, erosion and redeposition directly determine the lifetime of plasma-facing components (PFCs) as well as the availability of fusion devices and thus are crutial factors for economic operation of an upcoming fusion reactor. Meanwhile, these PWI processes are strongly linked to edge plasma flux and fluence.[4] Therefore, the key challenge for PWI studies in long-pulse operation is to monitor the elemental composition on the surface of the PFCs as well as the edge plasma condition during experimental processes in fusion device *in situ* and real-time. Post-mortem analysis has been largely employed in the past, hindering a direct comparison of plasma conditions with surface conditions on a time scale of less than many seconds of plasma exposure if limiter locks are used.[5]

The Experimental Advanced Superconducting Tokamak[6] (EAST), which is the world's first fully superconducting magnetic confinement facility with ITER-like magnetic field configuration, has achieved a stable 101.2 s steady-state high confinement plasma (H-mode), setting a world record in long-pulse H-mode operation on July 3rd, 2017.[7] Therefore, EAST provides a unique platform to investigate the physical and engineering issues of PWI research for the next H-mode long-pulse fusion devices such as ITER, the upcoming China Fusion Engineering Test Reactor (CFETR)[8] and beyond.

Laser-induced breakdown spectroscopy (LIBS) as a well-established elemental composition analysis method has been proposed and demonstrated as one of the most promising methods for *in situ* PWI studies on the first wall of fusion devices.[9,10] Several post-mortem setups in the labs[11–16] and *in situ* proof-of-concept studies[17,18] on PFCs have demonstrated that LIBS technique has the excellent capability for *in situ* operation in fusion devices. Therefore, the LIBS technique can provide a unique tool for PWI researches such as fuel retention and material deposition under long-pulse plasma operation in EAST. For this purpose, it is essential to not only measure the elemental composition of PFCs by LIBS but also simultaneously monitor the local edge plasma conditions near PFCs during long-pulse discharges. Thus, a timing system, which can synchronize EAST discharges with the trigger and delay of laser and spectrometers for both LIBS and optical emission spectroscopy (OES) measurements, is a key prerequisite for the application of *in situ* LIBS diagnostic system under long-pulse plasma operation in EAST. In addition, the timing system must be flexible and adjustable to enable changes of sequences and measurement schemes for LIBS pulses for the different experimental conditions.

In the present study, it is the first time that an *in situ* LIBS system combined with OES and flexible timing system is used to investigate PWI during long-pulse plasma operation in EAST. Preliminary results from EAST long-pulse plasma operation are shown to illustrate the relation between fuel retention on the first wall and local deuterium (D) particle fluence by analyzing LIBS combined with edge plasma OES. In addition, the plan of the upgraded LIBS system for divertor measurement in EAST is also proposed.

II. EXPERIMENT

EAST has ITER-like magnetic field configurations and heating schemes with dominant electron heating provided by radiofrequency (RF) wave heating. EAST was built to demonstrate high-power, long-pulse plasma operation. It has a major radius of 1.85 m, minor radius of 0.45 m, toroidal field ≤ 3.5 T and expected plasma pulse length up to 1000 s.[6,19] Molybdenum (Mo), tungsten and graphite were used as plasma-facing materials of the first wall, upper divertor and lower divertor, respectively. Furthermore, advanced wall conditioning techniques with lithiation by lithium (Li) evaporation as well as real-time injection of Li powder during discharges have been developed to reduce impurity radiation, particle recycling and H/(H+D).[20]

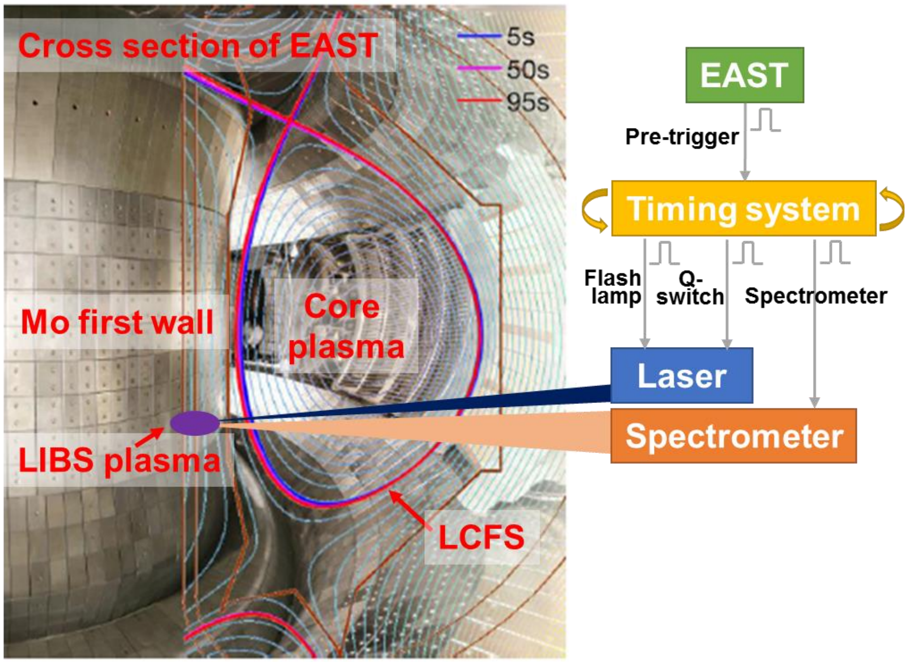

Fig. 1. The schematic view of cross section and working sequence of LIBS system, and positions of the last closed flux surfaces in a long-pulse discharge in EAST

The *in situ* LIBS system is located at the H-port, which is one of the 16 main horizontal ports along the toroid in EAST. The schematic of the system is illustrated in Fig. 1. The detail of the optical system can also be found in our previous works.[11,21] A nanosecond pulsed Q-switched Nd:YAG laser (Brilliant Eazy, Quantel) at a wavelength of 1064 nm and a maximum energy of 330 mJ is used to ablate the target and produce the LIBS plasma. The fiber-coupled detectable area of the LIBS system is located on the high-field side (HFS) near mid-plane. It covers more than 12 × 12 cm^2 and two standard Mo tiles which are named H8I3 and H8I4. Scanning of laser spot and observation optics is achieved by using motorized mirror holders. The laser focusing lens and the signal collecting lens are located outside EAST vessel and about 3 m away from the detectable first wall. The signal light is coupled into fiber bundles which can couple to spectrometers on the other side of the fibers. Two different spectrometers can be switched flexibly according to the experimental conditions. The first spectrometer is a multi-channel spectrometer (LIBS2500+, Ocean Optics) in a wide wavelength range from 200 – 980 nm. The second spectrometer is a high throughput, high sensitivity spectrometer (HoloSpec F/1.8i, Andor) with gated ICCD camera (iStar 340, Andor) which covers a wavelength range of 634 – 672 nm with a full-width half-maximum (FWHM) resolution of 0.09 nm. Both spectrometers have enough spectral resolution to distinguish hydrogen (H) and D in the Balmer-alpha-line.

During the EAST long-pulse plasma discharges, the spectrometer is used for measuring the OES from the edge plasma to analyze the edge plasma conditions and provide integral photon flux of the Dα line emission. As shown in Fig. 1, the optical collection path for OES is identical to the optical collection path of the LIBS which is optimized and focused on the LIBS plasma location near the first wall. The f-number for optical collection is about 22. Therefore, the observation path, as depicted in Fig. 1, passes through the last closed flux surface (LCFS) two times at both the high and low magnetic field side. Most of the D, Li atoms and Li ions in lower charge states emit light in a volume near the LCFS during the tokamak discharge.[22] Although both sides could have contributions to the OES signal in visible range from D and Li, the emission from the neutral particles is mainly from the HFS. This is due to three factors: First, more particle collision and charge-exchange reactions occur near the first wall. Second, there is no PFC near the low magnetic field side from the OES collecting view due to the large flange of the H-port. Third, the focal point of the optical collecting system is near the HFS. These factors result in an optical collection mainly occurring near the HFS.

The timing system is a key device to synchronize and control the trigger and delay time for each LIBS and OES measurement with a resolution of 1μs, using a base clock of 40 MHz. In the long-pulse operation of EAST, the timing system must have the ability to allow experiments for the different discharge duration times and enable flexible measurements with various laser and spectrometer triggers. The hardware of the timing system is made up by a multi-function RIO module with field programmable gate array chip (PXI-7833R, National Instruments), a shielded I/O connector block (SCB-68, National Instruments) and a compact computer (PXI-8106, National Instruments) which is mounted in a compact rack (PXI-1031, National Instruments). A LabVIEW program is developed and used to control the programmable RIO module, allowing for all time critical tasks triggered via the standard transistor-transistor logic (TTL) signal and thus ensuring synchronization to EAST operation.

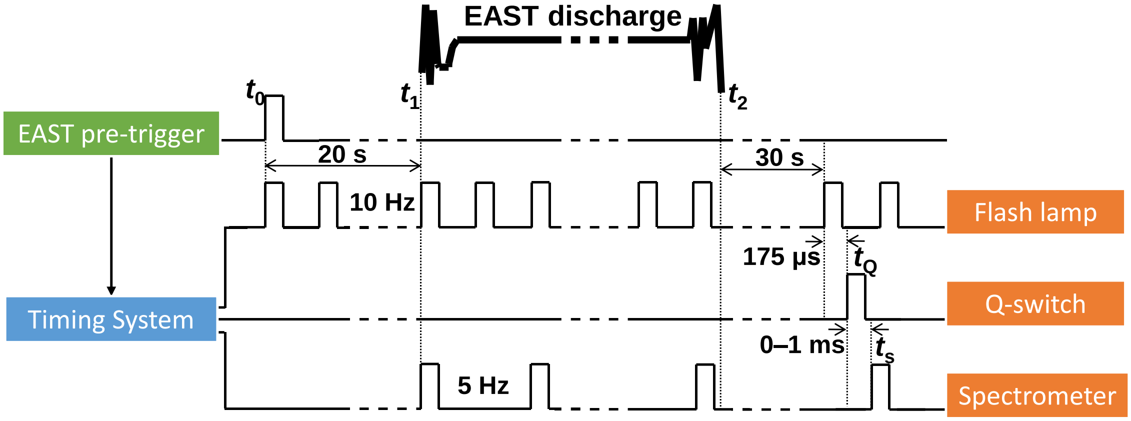

Fig. 2. The time sequence of the LIBS experiment under long-pulse operation in EAST

A schematic of the LIBS and OES timing sequences is shown in Fig. 2. The laser flash lamp and Q-switch as well as the spectrometer are set to external trigger mode and triggered by the timing system. The EAST discharge pre-trigger TTL signal which is 20 s ahead of each discharge is used to start the timing system. Then, an initial TTL signal with 10 Hz repetition rate is generated at t_0 to trigger the operation of flash lamp to make sure that the flash lamp and the laser system are in stable operating conditions. After a delay time of 20 s, a TTL signal with 5 Hz is generated at t_1 which is the start time of EAST discharge to trigger the spectrometer and measure the OES spectra from edge plasma until the end of the EAST discharge, denoted by t_2. The delay time between t_1 and t_2 is set by the program and depends on the time duration of discharge which is set in the range from 10 – 100 s in the long-pulse H-mode operation of EAST in 2017 experimental campaign. After the EAST discharge, a TTL signal at 5 Hz is generated at t_Q to trigger the Q-switch of laser and fire the laser to ablate the target on the first wall. The delay time between t_2 and t_Q is set about 30 s to keep the EAST chamber background pressure stable between LIBS measurements. The Q-switch of laser can also be triggered during the EAST discharge to achieve the laser-induced ablation spectroscopy measurement. [21,23] Laser output energy can be adjusted by the delay between flash lamp and Q-switch. It is set to 175 μs for the maximum energy output. The number of the Q-switch triggers which decide the successive number of laser pulses is dependent on the required ablation depth in the depth analysis of LIBS. When only the surface of the first wall is measured, the number of the Q-switch trigger is set to 1 and only a single laser shot is fired on the first wall. In order to obtain the LIBS plasma emission, a TTL with 5 Hz is generated at t_s to trigger the spectrometer with a fixed delay with respect to t_Q. The delay time between t_Q and t_s, LIBS delay time, can be set as 0 – 1 ms by the program to optimize the integral gate of exposure time and reduce the continuous radiation of LIBS plasma.

In addition, recorded spectra are analyzed by a MATLAB data processing program automatically after the spectra acquisition. The spectral integral areas of Dα and Li peaks in OES and analyzed elemental peaks in the

LIBS are processed by peak fitting. Then, the intensities with discharge time, integral intensity for each discharge, as well as elemental depth profile of LIBS are obtained.

III. RESULTS AND DISCUSSION

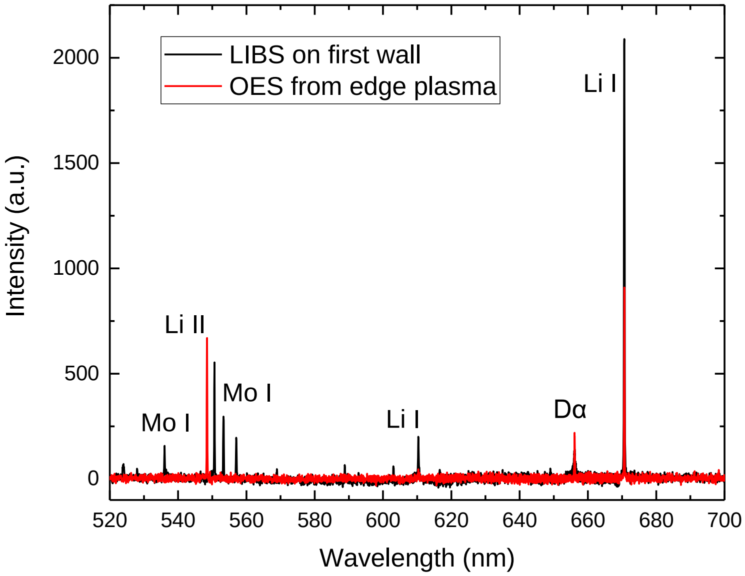

Fig. 3. Typical LIBS spectrum obtained from the first wall and OES spectrum observed from edge plasma in EAST

The typical spectra of LIBS on the Mo first wall and OES from edge plasma by using the *in situ* LIBS system with the timing system in EAST 2017 campaign are shown in Fig. 3. The exposure times for both spectra are 1 ms. The LIBS delay time is set to 0 to collect all the LIBS plasma emissions. The LIBS spectrum (shown in black) is measured after Li wall conditioning and D discharge by using single pulse LIBS on the surface of mid-plane Mo first wall. It clearly shows Li emission, Dα emission from fuel retention as well as Mo atomic line emission from the first wall substrate. The H content in the core discharge plasma is very low due to the Li wall conditioning[24], thus the fuel retention on the wall is dominated by D implantation and codeposition. The H emission is lower than the limitation of detection of spectrometer in these experimental conditions. The bremsstrahlung with continuous background radiation due to high laser plasma temperature and density is subtracted in the LIBS spectrum. Li atom and ion as well as Dα peaks are observed in the edge plasma OES spectrum. Some emission lines of Mo impurity from first wall erosion may be observed in some cases of edge localized modes burst or fast plasma shutdown. The emission intensity ratio of Li II and Li I in edge plasma OES is much higher than it in the LIBS due to a higher ionization and excitation rates in the edge plasma.

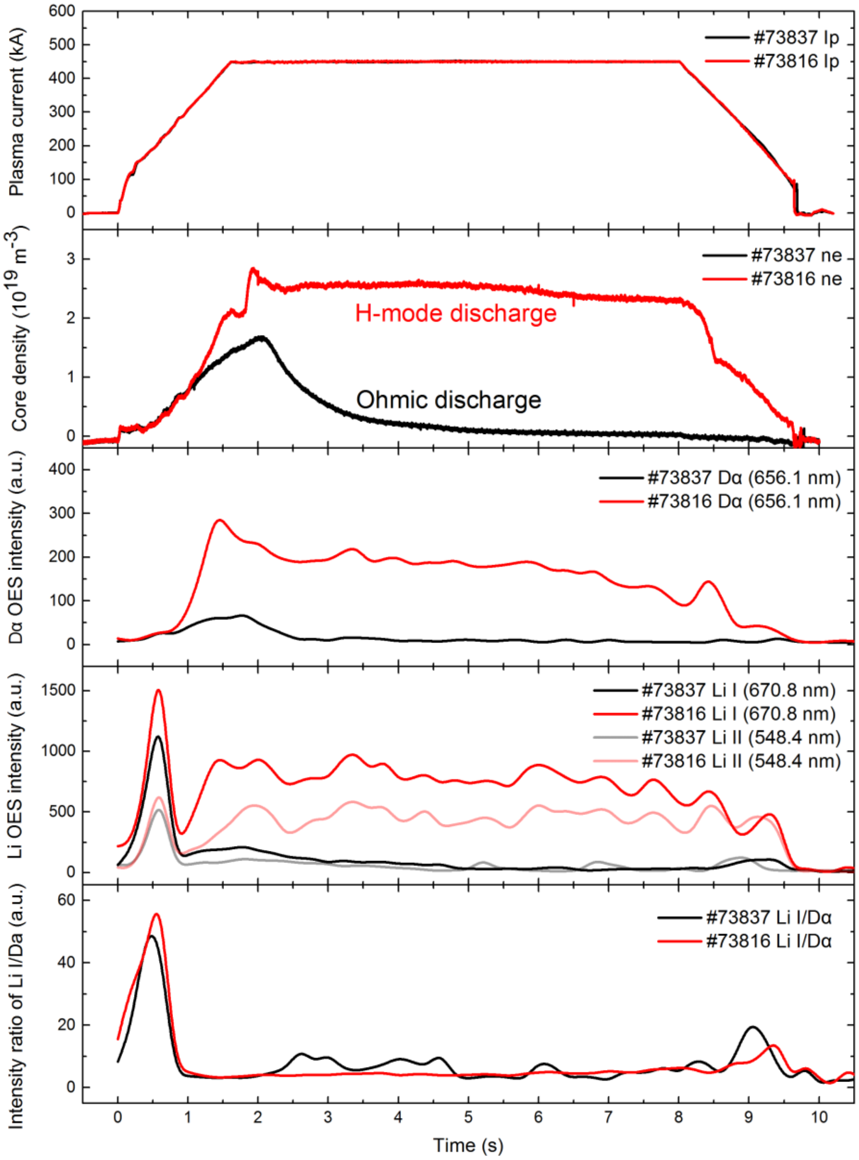

Fig. 4. Typical data of OES intensities from edge plasma in an H-mode discharge and an ohmic discharge

The plasma currents, core plasma densities, intensities of Dα (656.1 nm), Li I (670.8 nm) and Li II (548.4 nm) and intensity ratios of Li I/ Dα in the discharges of #73837 and #73816 are shown in Fig. 4. The OES spectra are obtained with an exposure time of 1 ms and an acquisition frequency of 5 Hz during the 10 s EAST discharges. #73816 is a 10 s duration discharge with H-mode from 1.8 s to 8.4 s. The RF heating includes lower hybrid wave (LHW) of 1.8 MW and electron cyclotron resonance heating (ECRH) of 0.35 MW. #73837 is a 10 s duration ohmic discharge without RF heating. Its averaged ohmic power is about 0.15 MW which is much lower than the total input power in #73816. Before the discharges of #73816 and #73837, the wall has exposed to about 200 s and 500 s plasma after a routine Li wall conditioning with Li evaporator, respectively. During the first second of the discharge, part of the first wall at the HFS acts as a limiter during the limiter startup phase of EAST. The edge plasma can directly interact with the first wall and result in Li sputtering into the edge plasma and significant Li radiation in both ohmic and H-mode discharges. Due to the much higher input power, the edge particle flux in #73816 H-mode discharge is much higher than that in #73837 ohmic discharge. Therefore, the emission intensities of Li I, Li II and Dα in edge plasma of #73816 H-mode discharge are also much higher. The intensity ratio of Li I/Dα which is proportional to the flux ratio in the discharges of #73816 is more stable than it in #73837 during discharge.

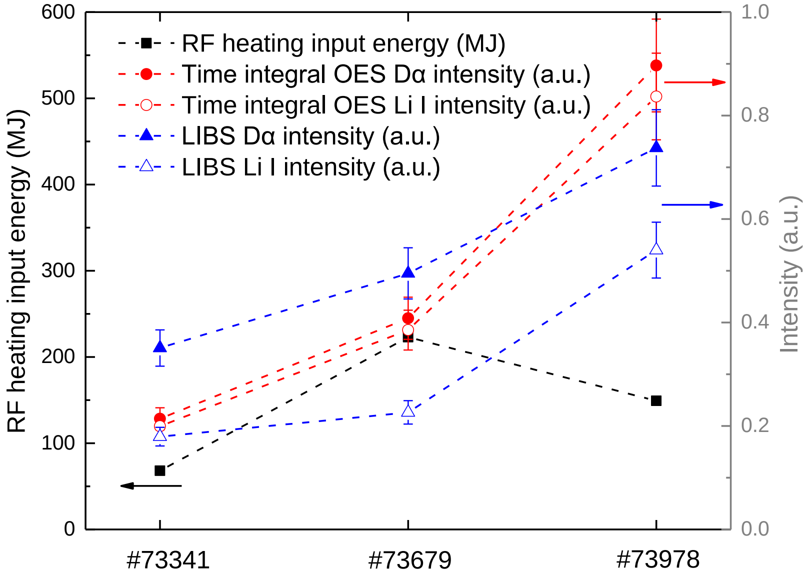

Fig. 5. Comparison of LIBS intensity on the first wall and edge plasma OES in different long-pulse discharges

One of the most important purposes of this work is to illustrate the relation between D retention on the first wall and edge particle fluence and investigate the PWI process during long-pulse discharges in EAST. The input energies of RF heating, time integral OES intensities, LIBS D and Li intensities of three long-pulse discharges with upper single-null of #73341, #73679 and #73978 are shown in Fig. 5. The discharge duration times for the three discharges are 20 s, 65 s and 50 s, respectively. The total input powers of RF heating are about 3.45 MW, 3.45 MW and 3 MW, respectively. The total input energies of RF heating are shown in Fig. 5 (in black). The core plasma densities are 2.8×10^{19} m^{-3}, 3.1×10^{19} m^{-3} and 3.0×10^{19} m^{-3}, respectively. The plasma currents are 450 kA, 450 kA and 400 kA, respectively. The distances between HFS and LCFS at mid-plane of the three discharges are about 5 cm.

The OES Dα intensity from the edge plasma is proportional to the local photon flux which can be converted to a particle flux via an inverse photon-efficiency S/XB coefficient.[25] Although the edge plasma perpendicularly transports to the mid-plane first wall due to the magnetic field constraint, the local flux of neutral particles which are induced by particle collision and charge-exchange is proportional to the edge plasma flux.[26] So in this work, the Dα intensity is as a proxy for qualitative analysis of the impinging particle flux on the first wall. The time integral intensities of Dα and Li I (670.8 nm) from OES which are proportional to particle fluences are obtained by integrating intensity of OES over time in Fig. 5 (in red). The time integral intensity corresponds to the particle fluence in the discharge. Unlike total input energies of RF heating, time integral intensities of Dα clearly show that $I_{D\alpha}$ (#73341) < $I_{D\alpha}$ (#73679) < $I_{D\alpha}$ (#73978). The LIBS intensities of Dα and Li I (610.4 nm) which are obtained on the first wall after the end of the discharges are shown in Fig. 5 (in blue). Each LIBS measurement area on the first wall is cleaned by the laser ablation to avoid the D accumulation from previous discharges. So the Dα intensity of LIBS only relates to the last discharge. The LIBS depth analysis shows that the D signal only exists in the first laser pulse in the experimental conditions. So single pulse LIBS on the surface is utilized to measure the fuel retention amount on the wall. The LIBS Dα intensities in the three discharges show that $I_{D\alpha}$ (#73341) < $I_{D\alpha}$ (#73679) < $I_{D\alpha}$ (#73978) which shows the same trend as the time integral intensities. Thus, the correlation between LIBS intensities of Dα from LIBS on first wall material and time integral intensities of Dα from edge OES is clearly demonstrated, indicating that the retention in the PFCs increases as particle fluence to the wall increases. We conclude that the fuel retention on the first wall is dominantly influenced by the local D particle fluence in the present experimental conditions. The presence of Li emission in the LIBS indicates that codeposition of Li-D is a likely candidate for the retention mechanism on the HFS first wall.

IV. CONCLUSIONS AND FUTURE WORK

An *in situ* LIBS diagnostic system combined with an edge plasma OES system and a flexible timing system has been developed for *in situ* PWI studies during long-pulse plasma operation in EAST. The timing system controls not only the external triggers of laser flash lamp, Q-switch and spectrometer but also the sequence and time delay to successfully control the edge plasma OES and first wall LIBS measurements. The OES spectra show D and Li emissions from the edge plasma transport. The spectral intensities in the H-mode discharge are much stronger than in ohmic discharges without RF heating. The OES Dα signal intensity and its time integral intensity allow to investigate the relative behavior of local particle flux and fluence during discharges. The LIBS spectra from the first wall show a significant potential to identify the elements of fuel and Li coming from wall conditioning. Relative quantitative analysis of the signal intensities has been demonstrated in this work. The preliminary results of fuel retention on the first wall show that the D retention amount increases as the local edge D particle fluence increases in the long-pulse plasma discharges. Based upon the Li emission observed in the LIBS in conjunction with Dα emission, it is likely that Li-D codeposition is the main source of retention.

In the future, the local edge particle fluence will be quantified by considering S/XB coefficient and measuring the plasma temperature and density in the edge region. Quantitative analysis by LIBS with radiometrically calibrated spectrometry will be compared to the edge plasma conditions and provide more information to *in situ* study PWI physical processes under the long-pulse operation in EAST. The retention as a function of the distance between HFS and LCFS will be studied to search for a transition for the retention behavior in the transition from net erosion to net deposition zone at the HFS first wall. In addition, it is planned to use an endoscope system to upgrade and extend the LIBS and OES detectable area to the upper divertor region which is a strong interaction zone for PWI study. The wall Langmuir probe and infrared camera observation systems will be used to achieve a characterization of edge plasma conditions and wall surface temperature. Deposition and erosion in divertor zones will be *in situ* investigated by using the upgrade LIBS system in EAST for PWI research in long-pulse operation.

ACKNOWLEDGMENTS

This work was supported by the National Science Foundation of China (Nos. 11605023, 11605238, 11705020, 11475039) and the National Magnetic Confinement Fusion Science Program of China (No. 2013GB109005), Chinesisch-Deutsches Forschungs project (No.GZ768), China Postdoctoral Science Foundation (Nos. 2017T100172, 2016M591423). This work has been carried out within the framework of the EUROfusion Consortium and has received funding from the Euratom research and training programme 2014-2018 under grant agreement No 633053. The views and opinions expressed herein do not necessarily reflect those of the European Commission. We would like to acknowledge the supports and contributions from the rest of the EAST team and collaborators.

REFERENCES

[1]http://www.iter.org

[2]J. Roth, E. Tsitrone, A. Loarte, Th. Loarer, G. Counsell, R. Neu, V. Philipps, S. Brezinsek, M. Lehnen, P. Coad, Ch. Grisolia, K. Schmid, K. Krieger, A. Kallenbach, B. Lipschultz, R. Doerner, R. Causey, V. Alimov, W. Shu, O. Ogorodnikova, A. Kirschner, G. Federici, A. Kukushkin, J. Nucl. Mater. **390–391**, 1–9 (2009).

[3]S. Brezinsek, T. Loarer, V. Philipps, H.G. Esser, S. Grünhagen, R. Smith, R. Felton, J. Banks, P. Belo, A. Boboc, J. Bucalossi, M. Clever, J.W. Coenen, I. Coffey, S. Devaux, D. Douai, M. Freisinger, D. Frigione, M. Groth, A. Huber, J. Hobirk, S. Jachmich, S. Knipe, K. Krieger, U. Kruezi, S. Marsen, G.F. Matthews, A.G. Meigs, F. Nave, I. Nunes, R. Neu, J. Roth, M.F. Stamp, S. Vartanian, U. Samm, and JET EFDA contributors, Nucl. Fusion. **53**, 083023 (2013).

[4]Y. Liang, O. Neubauer, R. König, M. Krychowiak, B. Schweer, P. Denner, M. Rack, D. Reiter, Y. Feng, A. Krämer-Flecken, P. Drews, F. Hasenbeck, S. Liu, Y. Gao, E.H. Wang, Y. Wei, M. Dostal, L. Li, N. Wang, J. Geiger, Y. Suzuki, S. Sereda, P. Börner, A.C. Weger, W. Biel, S. Brezinsek, A. Charl, G. Czymek, D. Höschen, F. Effenberg, O. Grulke, D. Nicolai, H.T. Lambertz, O. Marchuk, O. Schmitz, K.P. Hollfeld, M. Knaup, G. Offermanns, G. Satheeswaran, A. Terra, J. Thomas, T. S. Pederson, U. Samm, C. Linsmeier, and the W7-X team, Nucl. Fusion **57**, 066049 (2017).

[5]B. Schweer, S. Brezinsek, H. G. Esser, A. Huber, Ph. Mertens, S. Musso, V. Philipps, A. Pospieszczyk, U. Samm, G. Sergienko, and P. Wienhold, Fusion Sci. Technol., **47**, 138–145 (2005).

[6]J. Li, H. Guo, B. Wan, X. Gong, Y. Liang, G. Xu, K. Gan, J. Hu, H. Wang, L. Wang, L. Zeng, Y. Zhao, P. Denner, G. Jackson, A. Loarte, R. Maingi, J. Menard, M. Rack, and X. Zou, Nat. Phys. **9,** 817–821 (2013).

[7]Y. Liang *et al*., "Recent advances in EAST physics experiments towards high-performance steady-state H-mode operation", 1st Asia-Pacific Conference on Plasma Physics 2017.

[8]Y. Wan J. Li, Y. Liu, X. Wang, V. Chan, C. Chen, X. Duan, P. Fu, X. Gao, K. Feng, S. Liu, Y. Song, P. Weng, B. Wan, F. Wan, H. Wang, S. Wu, M. Ye, Q. Yang, G. Zheng, G. Zhuang, Q. Li, and CFETR team, Nucl. Fusion **57,** 102009 (2017)

[9] V. Philipps, A. Malaquias, A. Hakola, J. Karhunen, G. Maddaluno, S. Almaviva, L. Caneve, F. Colao, E. Fortuna, P. Gasior, M. Kubkowska, A. Czarnecka, M. Laan, A. Lissovski, P. Paris, H.J. van der Meiden, P. Petersson, M. Rubel, A. Huber, M. Zlobinski, B. Schweer, N. Gierse, Q. Xiao, and G. Sergienko, Nucl. Fusion **53**, 093002 (2013).

[10] C. Li, C. Feng, H. Oderji, G. Luo, and H. Ding, Front. Phys. **11**, 114214 (2016).

[11] C. Li, D. Zhao, Z. Hu, X. Wu, G. Luo, J. Hu, and H. Ding. Nucl. Mater. **463**, 915–918 (2015).

[12] A. Semerok, D. L'Hermite, J. Weulersse, J. Lacour, G. Cheymol, M. Kempenaars, N. Bekris, and C. Grisolia, Spectrochim. Acta Part B **123**, 121–128 (2016).

[13] J. Karhunen, A. Hakola, J. Likonen, A. Lissovski, M. Laan, P. Paris, and JET EFDA Contributors, J. Nucl. Mater. **463**, 931–935 (2015).

[14] P. Paris, K. Piip, A. Hakola, M. Laan, M. Aints, S. Koivuranta, J. Likonen, A. Lissovski, M. Mayer, R. Neu, V. Rohde, K. Sugiyama, and ASDEX Upgrade Team, Fusion Eng. Des. **98–99**, 1349–1352 (2015).

[15] Q. Xiao, R. Hai, H. Ding, A. Huber, V. Philipps, N. Gierse, and G.Sergienko, J. Nucl. Mater. **463**, 911–914 (2015).

[16] C. Li, N. Gierse, J. Oelmann, S. Brezinsek, M. Rasinski, C. Dhard, T. Sunn Pedersen, R. König, Y. Liang, H. Ding, Ch. Linsmeier, and the W7-X team, Phys. Scr. **T170**, 014004 (2017).

[17] G. Maurya, R. Kumar, A. Kumar, and A. Rai, Rev. Sci. Instrum. **86**, 123112 (2015).

[18] B. López-Miranda, B. Zurro, A. Baciero, and M. Martínez, Rev. Sci. Instrum. **87**, 11D811 (2016).

[19] B. Wan, J. Li, H. Guo, Y. Liang, G. Xu, L. Wang, X. Gong, and A. Garofalo, Nucl. Fusion **55**, 104015 (2015).

[20] J. Hu, Z. Sun, H. Guo, J. Li, B. Wan, H. Wang, S. Ding, G. Xu, Y. Liang, D. Mansfield, R. Maingi, X. Zou, L. Wang, J. Ren, G. Zuo, L. Zhang, Y. Duan, T. Shi, L. Hu, and EAST team, Phys. Rev. Lett. **114**, 055001 (2015).

[21] Z. Hu, N. Gierse, C. Li, P. Liu, D. Zhao, L. Sun, J. Oelmann, D. Nicolai, D. Wu, J. Wu, H. Mao, F. Ding, S. Brezinsek, Y. Liang, H. Ding, G. Luo, C. Linsmeier and EAST team, Phys. Scr. **T170**, 014046 (2017).

[22] C. Sang, , H. Du, G. Zuo, X. Bonnin, J. Sun, L. Wang, and D. Wang, Nucl. Fusion **56,** 106018 (2016).

[23] N. Gierse, S. Brezinsek, J. Coenen, T. Giesen, A. Huber, M. Laengner, S. Möller, M. Nonhoff, V. Philipps, A Pospieszczyk, B. Schweer, G. Sergienko, Q. Xiao, M. Zlobinski, U. Samm, and the TEXTOR Team, Phys. Scr., **T159,** 014054 (2014).

[24] G. Zuo, J. Hu, J. Li, Z. Sun, D. Mansfield, and L. Zakharov, J. Nucl. Mater. **438,** S90–S95 (2013).

[25] V. Winters, S. Brezinsek, F. Effenberg, M. Rasinski, O. Schmitz, L. Stephey, C. Biedermann, C. Dhard, H. Frerichs, J. Harris, M. Krychowiak, R. König, T. Sunn Pedersen, G. Wurden, and the W7-X team, Phys. Scr. **T170**, 014050 (2017).

[26] S. Brezinsek, G Sergienko1 A Pospieszczyk, Ph. Mertens, U. Samm, and P. Greenland, Plasma Phys. Control. Fusion, **47**, 615–634 (2005).